that dopant aggregation, caused by temperature instabilities in the island region during the crystal growth, is the origin of the island-like domains. A gradual transition from sharp to diffuse domain boundaries is again evident in Q and f_0 profiles at $z = 73$ μm (Fig. 3B), and the domain structure gradually loses its original periodicity approaching the island domain. For stable growth, the periodic modulation of dopant level should have a single frequency (which is the frequency of crystal rotation) (*1*, *8*), whereas disturbances in the system, such as melt or air convection and power fluctuations, may introduce additional modulations with different frequencies. When these additional frequencies are close to the crystal rotation frequency (with a period of ~7 μm in Fig. 3), interference eventually drives the solid-liquid interface out of stability, causing dopant aggregation and island domain formation during crystal growth (Fig. 3B).

A "butterfly" image of the dielectric constant is an indication of a lattice "edge dislocation" defect (Fig. 4A). The large difference in dielectric constant adjacent to the dislocation is caused by compressive and tensile stresses in lattice structure induced by the dislocation. The stress-induced ε contour is qualitatively consistent with the theoretical prediction for a lattice "edge dislocation" defect (*13*). The ε profile of a line scan along the z axis at $x = 38.7$ μm (Fig. 4B), which cuts through regions with compressive and tensile stresses, shows large opposite changes in ε on either side of the edge defect. This profile also indicates that our spatial resolution in this configuration (mainly limited by the radius of the tip) is better than 1 μm, because between the two points (0.6 μm apart), ε changed from the minimum to near maximum. Lattice dislocations in $LiNbO_3$ crystals are not observable by optical microscopy with polarized light because of the crystal's large birefringence.

REFERENCES AND NOTES

1. D. Feng and N. B. Ming, *Appl. Phys. Lett.* **37**, 607 (1980).
2. N. B. Ming *et al.*, *J. Mater. Sci.* **17**, 1663 (1982); G. A. Magel *et al.*, *Appl. Phys. Lett.* **56**, 108 (1990); Y. L. Lu and N. B. Ming, *ibid.* **69**, 1660 (1996).
3. J. A. Armstrong and N. Bloembergen, *Phys. Rev.* **127**, 1918 (1962).
4. See, for example, S. D. Cheng, Y. Y. Zhu, Y. L. Lu, N. B. Ming, *Appl. Phys. Lett.* **66**, 291 (1995), and references therein.
5. T. Ozaki *et al.*, *J. Appl. Phys.* **80**, 1697 (1996); R. LeBihan and M. Maussion, *J. Phys.* **33**, C2-215 (1972); P. J. Lin *et al.*, *Philos. Mag. A* **48**, 251 (1983); F. Saurenbach and B. D. Terris, *Appl. Phys. Lett.* **56**, 1703 (1990).
6. T. Wei, X. D. Xiang, P. G. Schultz, *Appl. Phys. Lett.* **68**, 3506 (1996).
7. Y. L. Lu, Y. Q. Lu, N. B. Ming, *ibid.*, p. 2781.
8. Y. L. Lu, L. Mao, N. B. Ming, *ibid.* **59**, 516 (1991).
9. H. A. Bethe and J. Schwinger, *Perturbation Theory of Cavities* (National Defense Research Committee, Washington, DC, 1943), pp. D1–117.
10. C. Gao, F. Duewer, X.-D. Xiang, in preparation.
11. J. Chen, Q. Zhou, J. F. Hong, W. S. Wang, D. Feng, *J. Appl. Phys.* **66**, 336 (1989).
12. Y. L. Lu, Y. Q. Lu, N. B. Ming, *Appl. Phys. Lett.* **68**, 2642 (1996), and references therein.
13. J. P. Hirth and J. Lothe, *Theory of Dislocations* (Krieger, Malabar, FL, ed. 2, 1992).

14. This work was supported by the director of Advanced Energy Projects Division, Office of Computational and Technology Research, U.S. Department of Energy, under contract DE-AC03-76SF00098.

14 January 1997; accepted 16 April 1997

Observation of Magnetic Domain Behavior in Colossal Magnetoresistive Materials With a Magnetic Force Microscope

Qingyou Lu, Chun-Che Chen, Alex de Lozanne*

Magnetic domain behavior was imaged in calcium-doped lanthanum manganese trioxide films. Magnetic domains behave differently at temperatures that are well below and near the Curie temperature T_c. At low temperatures the domains are very stable. As temperature rises toward T_c, domain-domain interactions become weaker and domains become highly mobile and subject to merging and splitting, yet the domains are still traceable. The contrast (which is a measure of magnetization) and size of domains continuously reduce to zero. The temperature at which the domains disappear agrees with the T_c obtained by a macroscopic magnetization measurement. Sample defects such as scratches tend to attract magnetic domains.

Metallic double-exchange ferromagnets, such as $LaMnO_3$ doped with doubly valenced impurities, were discovered and studied by Jonker and Van Santen in 1950 (*1*). Pure $LaMnO_3$ is an antiferromagnetic insulator with a well-known perovskite structure. When a divalent dopant D (D can be Ca, Sr, Ba, or Pb) is introduced, the $La_{1-x}D_xMnO_3$ that is generated exhibits paramagnetism at high temperatures and ferromagnetism at low temperatures for a wide doping range around $x = 1/3$. This phase transition has been commonly interpreted in terms of the double-exchange interaction model that was first proposed in 1951 (*2*). The substitution of La^{3+} by a D^{2+} cation results in a mixed Mn^{3+}/Mn^{4+} valence. The electron can hop from one Mn ion to another Mn ion through O^{2-} in between. Because Hund's rule must be obeyed on Mn sites, this hopping process can occur only when the ionic spins of two Mn ions are parallel. The motion of the electrons thus causes a partial alignment of the Mn spins that in turn lowers the kinetic energy and favors the occurrence of ferromagnetism. However, there are other results that do not support this model (*3*).

Another intriguing feature of doped $LaMnO_3$ is the magnetoresistive effect that was first measured on a flux-grown single crystal in 1969 (*4*). Shortly thereafter, the dependence of resistivity on temperature and the applied magnetic field was obtained by Kubo and Ohata by exploitation of the well-known Drude approximation in terms of a Kondo lattice with ferromagnetic coupling (*5*).

Although it has been studied for years, the behavior of doped $LaMnO_3$ is far from well understood and is still attracting extensive investigation because of its value in basic research as well as its possible application in magnetic recording. Whereas much attention has recently been paid to bulk magnetization and structural properties (*6*), we have been trying to understand the behavior of the local magnetization in thin films of this compound at the microscopic level. We used a low-temperature magnetic force microscope (LTMFM) to study the magnetic domain behavior in colossal magnetoresistive $La_{0.65}Ca_{0.35}MnO_3$ films.

The $La_{0.65}Ca_{0.35}MnO_3$ thin films were grown on $SrTiO_3(100)$ substrates by electron-beam and thermal co-evaporation (*7*) of the metallic elements in an oxygen partial pressure of 4×10^{-6} torr at a substrate temperature of 700°C. After deposition, ex situ annealing was performed at 960°C in air for 30 min. The thickness of the films was 300 nm (*8*).

The dependence of sample resistivity ρ and magnetization M on temperature T in different magnetic fields H applied in the plane of the thin film (Fig. 1) shows the colossal magnetoresistance effect. Without

Department of Physics, University of Texas, Austin, TX 78712–1081, USA.

*To whom correspondence should be addressed. E-mail: lozanne@physics.utexas.edu

an external H field, the curve peaks at T_p = 277 K. When fields are applied, the peak shifts slightly but drops greatly. A paramagnetic-to-ferromagnetic phase transition is seen in the M-T data with a somewhat wide transition zone centered at 235 K. We define T_c as the temperature at which the sample just begins to become ferromagnetic, which is 245 K in this case. This T_c is also close to the T_p obtained from the ρ-T curve.

Our LTMFM has been described previously (9) and can operate at temperatures as low as 6 K. In the topographic mode, the tip contacts the sample with a typical force of 150 nN. We made the tip sensitive to magnetic forces by depositing a film of Co on it and magnetizing it along its axis. In the magnetic mode, the tip oscillates at an average distance of 570 nm above the surface (with feedback set to a force gradient of $\sim 2.4 \times 10^{-3}$ N/m). A quantitative calibration of the actual local field and its gradient is very difficult in MFM. We have looked at VHS tape under similar conditions and obtained images with somewhat lower contrast (9). The field is applied perpendicular to the thin film in all of the images shown here.

A magnetic image taken at 100 K (far below T_c = 245 K) in 38 G (field-cooled) is shown (Fig. 2A), and the topographic image for the same area is given (Fig. 2C). By comparing these two images, we see that the main features in the magnetic image have no counterparts in the topographic image, which means that the black and white features (Fig. 2A) come from a nonuniform magnetic field distribution and are therefore magnetic domains. It is likely that the magnetization of these domains is oriented parallel to the film, although in MFM one could get similar images with domains that are magnetized perpendicular to the film if the local field exceeds the coercivity of the magnetic particle on the tip. The domains are typically 6 μm long and 1 μm wide and are oriented along the (100) or (010) directions of the substrate (which are likely to be the same as that of the film because of epitaxy).

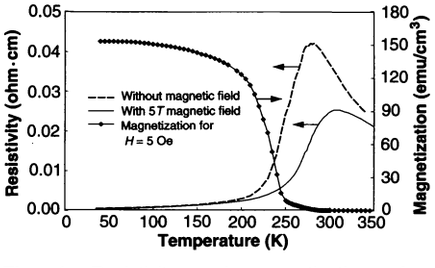

Fig. 1. Resistivity and magnetization of a $La_{0.65}Ca_{0.35}MnO_3$ thin film that is 300 nm thick. The field is applied parallel to the film.

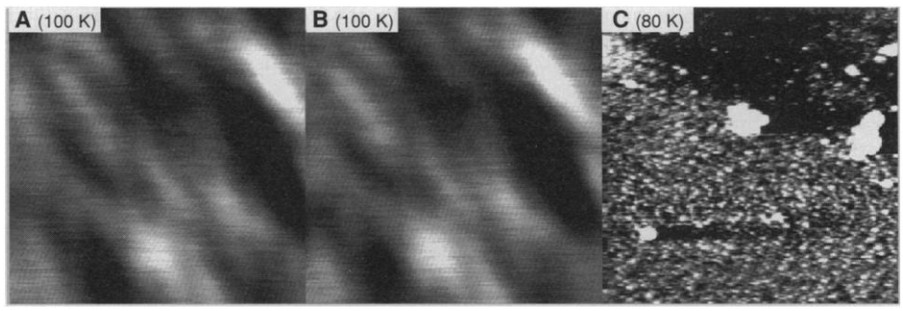

Fig. 2. (**A**) Magnetic image [12 μm by 14 μm by 25 nm (Δx by Δy by Δz, where z is normal to the surface)], of a $La_{0.65}Ca_{0.35}MnO_3$ thin film taken at 100 K in a 38-G field that is applied perpendicular to the film. (**B**) Same as (A), after the applied field was reversed. (**C**) Topographic image of the same area (11 μm by 12 μm by 23 nm) taken at 80 K.

The black and white domains are typically paired, which suggests that neighboring domains have opposite directions of magnetization. To check the strength of the domain-domain interactions, we switched the direction of the applied field and obtained a magnetic image (Fig. 2B). The similarity between Fig. 2B and Fig. 2A indicates that a field change from +38 G to −38 G is not sufficient to disturb the magnetic domains, which implies that there are strong interactions between domains. (We also cooled the sample in zero field to the same T range and obtained similar magnetic images.) We conclude that magnetic domains are spontaneously formed and cannot be easily disturbed, provided that the temperature is well below T_c.

Well below T_c, we generally did not see any movement or splitting of domains for fields up to 100 G, except for one example. A magnetic image taken at 104 K in a field of 55 G is shown in Fig. 3A, and after we temporarily increased the field to 100 G for 3 s and then reduced it to 45 G, we obtained the image shown in Fig. 3B. The domain marked with the arrow clearly splits into three. However, this 100-G field still could not make any domain move, which may imply that at low temperatures, it takes more energy to rearrange domains (that is, to move domains) than to split them.

As we increased T toward T_c, the domain-domain interactions became increasingly weaker, and the domains showed interesting responses (Fig. 4). All of these images were taken under the magnetic mode with one exception (Fig. 4I), a topographic image. We first cooled the sample to 77 K in zero field and warmed it up slowly to above T_c. Two domains at the lower left corner in Fig. 4A, which were originally separated at 180 K, moved toward each other and connected (Fig. 4C). This merged domain then moved upward, in an attempt to merge with the long dark object above it (Fig. 4D). They became connected (Fig. 4E) and then merged completely (Fig. 4F). As the temperature kept increasing, the early connected domain became narrower, shorter, and lighter, which shows that it became smaller and its magnetization was reducing continuously. It then disappeared (Fig. 4H), leaving only the long dark object that was present all the time. This "unknown object" is actually a scratch in the film, as is seen in the topographic image (Fig. 4I). The domains disappear at 244 K (see Fig. 4H) [near T_c = 245 K, which was obtained by the magnetization measurement (Fig. 1)], which confirms that

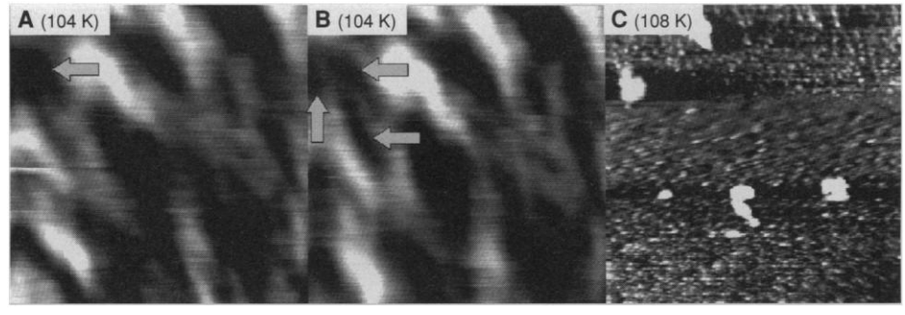

Fig. 3. (**A**) Magnetic image (12 μm by 14 μm by 25 nm) of a $La_{0.65}Ca_{0.35}MnO_3$ thin film taken at 104 K in a 55-G field. (**B**) Same as (A), after the applied field was increased to 100 G for 3 s and then reduced to 45 G. Arrows indicate the splitting of one domain into three. (**C**) Topographic image of the same area (12 μm by 15 μm by 25 nm) taken at 108 K.

the features were really magnetic domains.

The behavior of domains about the sample scratch is interesting and not well understood. We did similar imaging processes twice around the same scratch. In both cases, magnetic domains tended to move toward and merge with the scratch in spite of the fact that the domain shapes were different during these two processes (the domain-disappearance temperatures are the same). The boundary energy of the scratch may favor the merging.

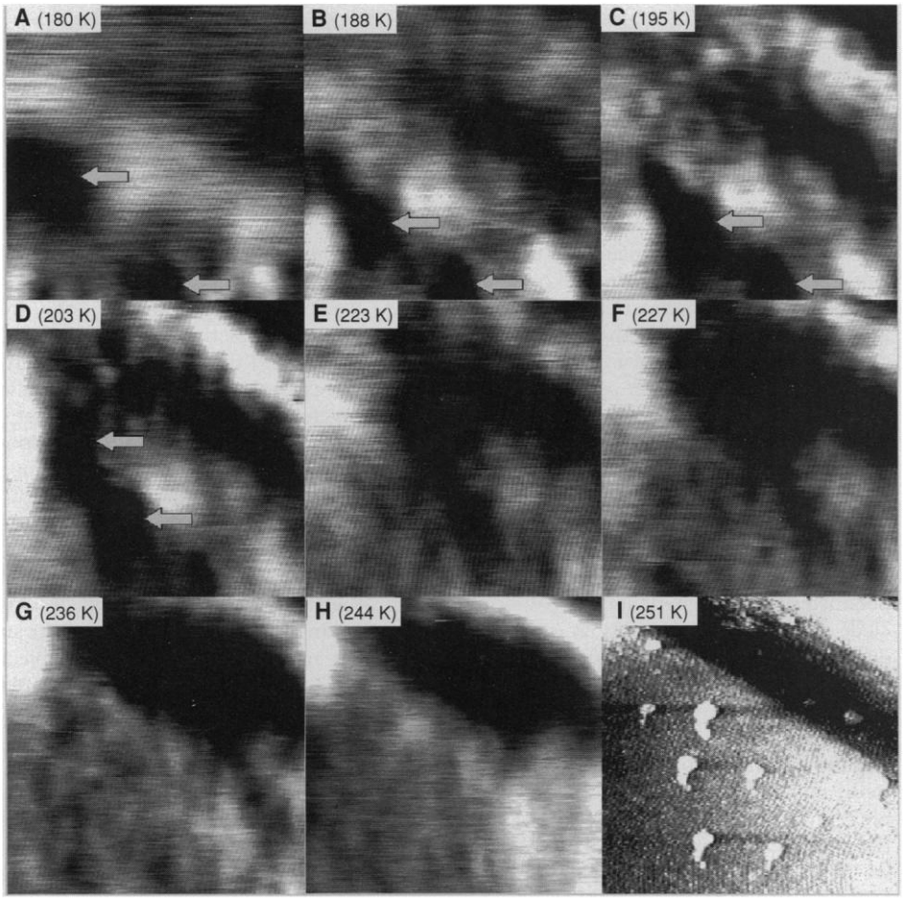

Fig. 4. Magnetic images of a $La_{0.65}Ca_{0.35}MnO_3$ thin film taken in zero applied field at increasing temperatures of (**A**) 180 K (16 μm by 22 μm by 38 nm), (**B**) 188 K (16 μm by 22 μm by 41 nm), (**C**) 195 K (17 μm by 25 μm by 43 nm), (**D**) 203 K (18 μm by 26 μm by 45 nm), (**E**) 223 K (21 μm by 30 μm by 52 nm), (**F**) 227 K (22 μm by 31 μm by 54 nm), (**G**) 236 K (23 μm by 33 μm by 57 nm), and (**H**) 244 K (24 μm by 35 μm by 60 nm). The images change in size because the piezoelectric coefficients of the scanner are temperature dependent. The last image (**I**) is the topography, taken at 251 K (25 μm by 36 μm by 63 nm). Arrows in (A) through (D) indicate the movement of domains.

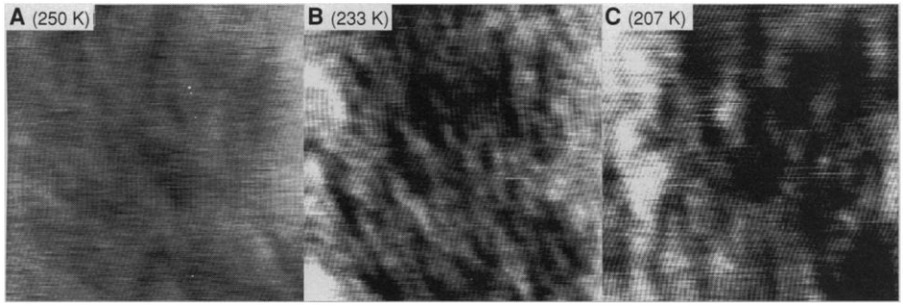

Fig. 5. Magnetic images taken in zero applied field at decreasing temperatures of (**A**) 250 K (25 μm by 36 μm by 52 nm), (**B**) 233 K (22 μm by 32 μm by 56 nm), and (**C**) 207 K (19 μm by 27 μm by 47 nm). The images change in size because the piezoelectric coefficients of the scanner are temperature dependent.

Figure 5 exhibits a reverse procedure in which the sample was cooled in zero field from above T_c to below T_c. The behavior of domains is somewhat different from that discussed above. The topography (not shown here) is similar to that shown in Fig. 4I but does not contain any large scratches. Above T_c, there was no evidence of magnetic domains (images not shown). Domains started to appear at 250 K (near T_c) (Fig. 5A). However, the domain contrast was small, which meant that there was a small domain magnetization. The contrast increased rapidly during cooling and became fairly clear at 233 K (Fig. 5B) and stronger at 207 K (Fig. 5C). At this time, domains showed extremely high mobility. Unlike the warming procedure presented in Fig. 4, it is now very difficult to trace the movement of any single domain in Fig. 5. Domains are everywhere, and they move, merge, and split randomly. This different behavior may be due to the lack of sample scratches, which probably serve as domain-pinning sites. The ability to image these domains opens many possibilities for the study of their detailed behavior as a function of temperature in any material with a magnetic transition below 400 K.

REFERENCES AND NOTES

1. G. H. Jonker and J. H. Van Santen, *Physica* **16**, 337 (1950); J. H. Van Santen and G. H. Jonker, *ibid.*, p. 599.
2. C. Zener, *Phys. Rev.* **82**, 403 (1951).
3. A. J. Millis *et al.*, *Phys. Rev. Lett.* **74**, 5144 (1995); H. Röder *et al.*, *ibid.* **76**, 1356 (1996); J. Zang *et al.*, *Phys. Rev. B* **53**, R8840 (1996).
4. C. W. Searle and S. T. Wang, *Can. J. Phys.* **47**, 2023 (1969).
5. K. Kubo and N. Ohata, *J. Phys. Soc. Jpn.* **33**, 21 (1972).
6. R. von Helmolt *et al.*, *Phys. Rev. Lett.* **71**, 2331 (1993); H.-Y. Hwang *et al.*, *ibid.* **75**, 914 (1995); P. G. Radaelli *et al.*, *ibid.*, p. 4488; A. Asamitsu *et al.*, *Phys. Rev. B.* **53**, R2952 (1996); R. H. Heffner *et al.*, *Phys. Rev. Lett.* **77**, 1869 (1996).
7. A. B. Berezin, C. W. Yuan, A. L. de Lozanne, *Appl. Phys. Lett.* **57**, 90 (1990).
8. The film structure was characterized by powder x-ray diffraction using Cu $K\alpha$ radiation, from which the film lattice constant c = 3.85(7)Å, with the c axis normal to the surface, is derived. The composition was determined by energy dispersion x-ray spectroscopy, which gives a doping rate of $x = 0.35 +/ -0.05$ and indicates Mn deficiency ($La_{0.65}Ca_{0.35}Mn_{0.8}O_3$). The oxygen concentration was nominal. The magnetization was measured by a Quantum Design (San Diego, CA) superconducting quantum interference device (SQUID) magnetometer. The resistivities were measured by the standard ac four-point method inside the magnetometer by means of platinum leads attached with pressed indium contacts.
9. C. W. Yuan, E. Batalla, A. de Lozanne, M. Kirk, M. Tortonese, *Appl. Phys. Lett.* **65**, 1308 (1994); C. W. Yuan *et al.*, *J. Vac. Sci. Technol. B* **14**, 1210 (1996).

10. We thank M. Tortonese of Park Scientific Instruments for providing piezoresistive cantilevers and J. T. Markert for the use of his SQUID magnetometer. Supported in part by the Texas Advanced Research and Technology Program.

26 December 1996; accepted 25 April 1997